

The voltage optimization of fast-timing MCP-PMT

Lingyue Chen^{a,b} and Sen Qian^{a,*} for the MCP-PMT workgroup

^a*Institute of High Energy Physics, Chinese Academy of Sciences,
100049 Beijing, China*

^b*School of Physical Sciences, University of Chinese Academy of Sciences,
100049 Beijing, China*

E-mail: qians@ihep.ac.cn

The microchannel plate (MCP) is used as the electron multiplier of the photomultiplier tube (PMT) for its excellent time performance. Researchers at IHEP have conceived a new type of 2-inch square shape 8×8 anodes Fast MCP-PMT (FPMT) with fast timing resolution for particle identification in the next generation of high-energy physics experiments and medical imaging equipment. Three samples of this FPMT were tested under different voltage between the photocathode and the MCP. The time resolution of the FPMT shows little influence with the change of the voltage, and the FPMT can reach a best transit time spread (TTS) of 30.7 ± 0.7 ps on average in single photoelectron (SPE) mode.

38th International Cosmic Ray Conference (ICRC2023)
26 July - 3 August, 2023
Nagoya, Japan



*Speaker

1. Introduction

The microchannel plate (MCP) is a special electron multiplier that utilizes its characteristic of secondary electron emission to amplify electrical signals. Compared to the conventional dynode chains, the small size of MCP considerably reduces the path length of the electron cascade through the detector, which ensures a good time resolution. Therefore, the MCP based photomultiplier tube (MCP-PMT) also has excellent time performance, which makes it a popular choice for weak light detection in various areas, including high-energy physics experiments [1], high-precision medical imaging devices [2], biofluorescence detection [3], and nucleic acid detection devices [4]. Led by the IHEP, CAS (Institute of High Energy Physics, Chinese Academy of Sciences) and cooperating with NNVT (North Night Vision Science & Technology Research Institute Co. Ltd), a series of MCP-PMT have been developed for the photon detection in particle physics and medical imaging. Among them the 20-inch Large MCP-PMT (LPMT) with small MCP units in the large area PMTs for the neutrino detection, which has been mass produced more than 15K pieces for the JUNO (Jiangmen Underground Neutrino Observatory) [5]. Based on this experience, a 2-inch square shape 8×8 anodes fast-timing MCP-PMT (FPMT) which is expected to be widely used in the next generation of high-energy physics experiments and medical imaging equipment [6]. Due to its common use in weak light detection, the single photoelectron (SPE) time resolution of FPMT has received great attention.

Transit time spread (TTS) is always considered as an important parameter to represent the time resolution of the PMT. As shown in Fig. 1, the TTS is almost determined by the transit time from the cathode to the first MCP, which can only be effected by the distance (d_1) and voltage (ΔV_1) between the cathode and the MCP [7]. To achieve a best time resolution possible, the distance was reduced as much as possible and the voltage divisions of the FPMT was adjusted to optimize the TTS. In this study, we tested three samples of the newly produced FPMTs under different voltage division to explore the impact of ΔV_1 to the time performance.

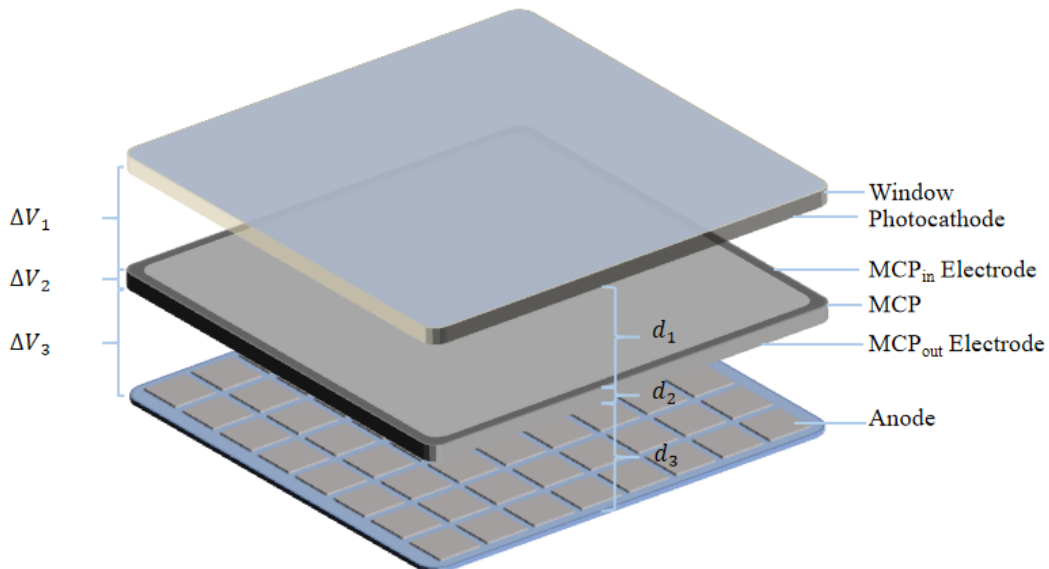


Figure 1: Schematic diagram of FPMT structure.

2. Material and method

2.1 Structure of FPMT

The FPMT is mainly composed of five parts, including the lead glass window, the bi-alkali photocathode, two chevron type MCPs, the anodes composed of 8×8 square pixel units for the position resolution, and the integrated ceramic shell. The external dimensions of the FPMT are $51 \times 51 \text{ mm}^2$. In order to improve the time resolution of the FPMT, both the distance from the photocathode to the MCP and the distance from the anode to the MCP are less than $300 \mu\text{m}$ [8].

As shown in Fig. 2, the voltage applied to the cathode-MCP (ΔV_1), MCP (ΔV_2) and MCP-anodes (ΔV_3) determine the TTS, gain and rise time (RT) of the FPMT respectively and can be adjusted by the parallel connection of different resistors. Therefore, the adjustment of the voltage division can always influence the performance of the FPMT. In this study, with ΔV_2 and ΔV_3 determined to ensure a gain of above 10^6 , ΔV_1 was increased from 110V to over 600V to explore its impact to the time performance of the FPMT, and three samples of this type of FPMT were tested.

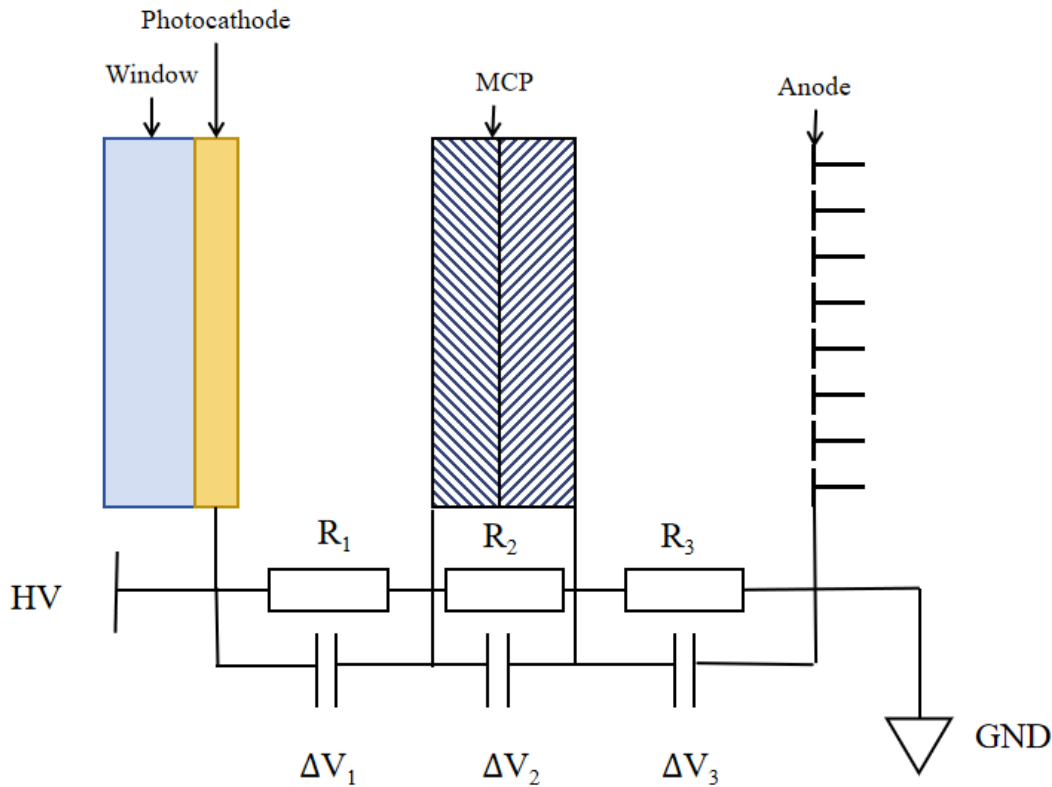


Figure 2: The divider circuit for the FPMT for general use.

2.2 Setup for measurement

Due to the fast-timing performance of the FPMT, the waveform sampling method is used to measure the TTS. A picosecond laser (PILAS DX NKT) with a time jitter less than 3 ps and a pulse width of 45 ps was chosen to limit the effect of light source. An optical attenuator was

used to attenuate the light intensity to single photon mode. In order to quickly acquire the ultra-fast waveforms of the FPMT, a LeCroy HDO9404 oscilloscope with a bandwidth of 4 GHz and a sampling rate of 40 GS/s was used as the data acquisition system, whose inter-channel jitter was less than 500 fs. As shown in Fig. 3, the measurement setup is the same as the previous setup [4, 9–12]. The picosecond laser provided a sync TTL signal input to the oscilloscope as the trigger signal, and the signal from the FPMT was input to another channel of oscilloscope as the tested signal. Through online statistics, the TTS spectrum in SPE mode was obtained by recording the transit time (TT) between trigger signal and the FPMT signal, with a 50% constant fraction discrimination (CFD) to locate the timing point. The standard deviation of the TT distribution is defined as TTS and is used to represent the time resolution of the FPMT. The SPE spectrum can also be obtained.

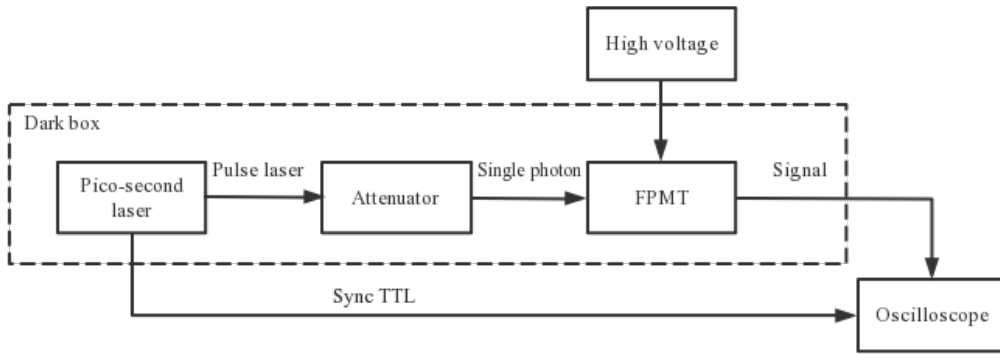


Figure 3: Setup of evaluation system.

3. Result

The typical SPE spectrum and TT spectrum in SPE mode of FPMT is shown in Fig. 4. The TT distribution consists of two Gaussian distributions, the one with higher counts represents the TT distribution of the photon signal from FPMT, while the other represents the TT distribution introduced by back-scattered electrons on the surface of MCP [13, 14]. The TT distribution is well fitted with the function:

$$f(x) = p(0)e^{-\frac{(x-p(1))^2}{2p(2)^2}} + p(3)e^{-\frac{(x-p(4))^2}{2p(5)^2}} \quad (1)$$

Where $p(0)$ is the maximum value of the first peak, $p(1)$ is the mean value of the first peak, and the $p(2)$ represents the TTS of this FPMT, $p(3)$ is the maximum value of the second peak, $p(4)$ is the mean value of the second peak, and the $p(5)$ represents the TTS of the back-scattered electron peak.

Fig. 5 shows the time resolution of two samples of the FPMT as a function of the voltage between the photocathode and the MCP (ΔV_1). As ΔV_1 increasing from 100V to 340V, the TTS maintained stability. However, when ΔV_1 keep increasing over 450V, the TTS rose rapidly. The

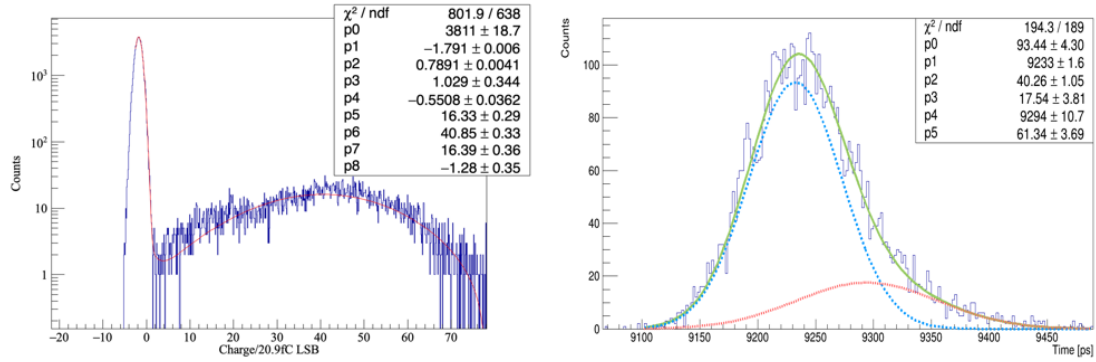


Figure 4: Typical SPE spectrum (left) and TT spectrum (right) of FPMT.

insensitivity of the time performance to the voltage division means that the distance between the photocathode and the MCP is small enough that the time performance can hardly be optimized by reducing the distance or adjusting the voltage division, and the abnormal change of TTS is due to the dark noise caused by the high operating voltage. Owing to its optimized structure, sample3 reached the best TTS and stability to ΔV_1 among the three FPMTs. Fig. 6 shows the TTS of sample3 and a single anode FPMT reported before [9] changed with ΔV_1 . The TTS of the single anode FPMT was slightly decreased with the increase of ΔV_1 , while the TTS of sample3 fluctuated around a certain value, which means that the close distance between the photocathode and the MCP makes the adjustment of ΔV_1 useless to optimize the time resolution. The best time resolution of sample3 obtained a TTS of 30.7 ± 0.7 ps on average at SPE mode.

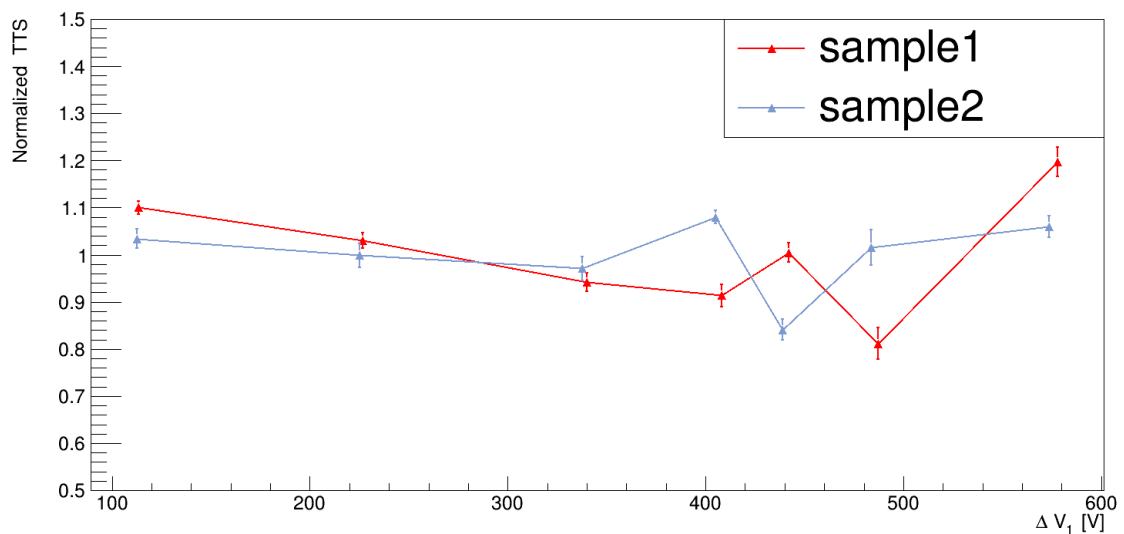


Figure 5: Normalized TTS of two samples changed with ΔV_1 .

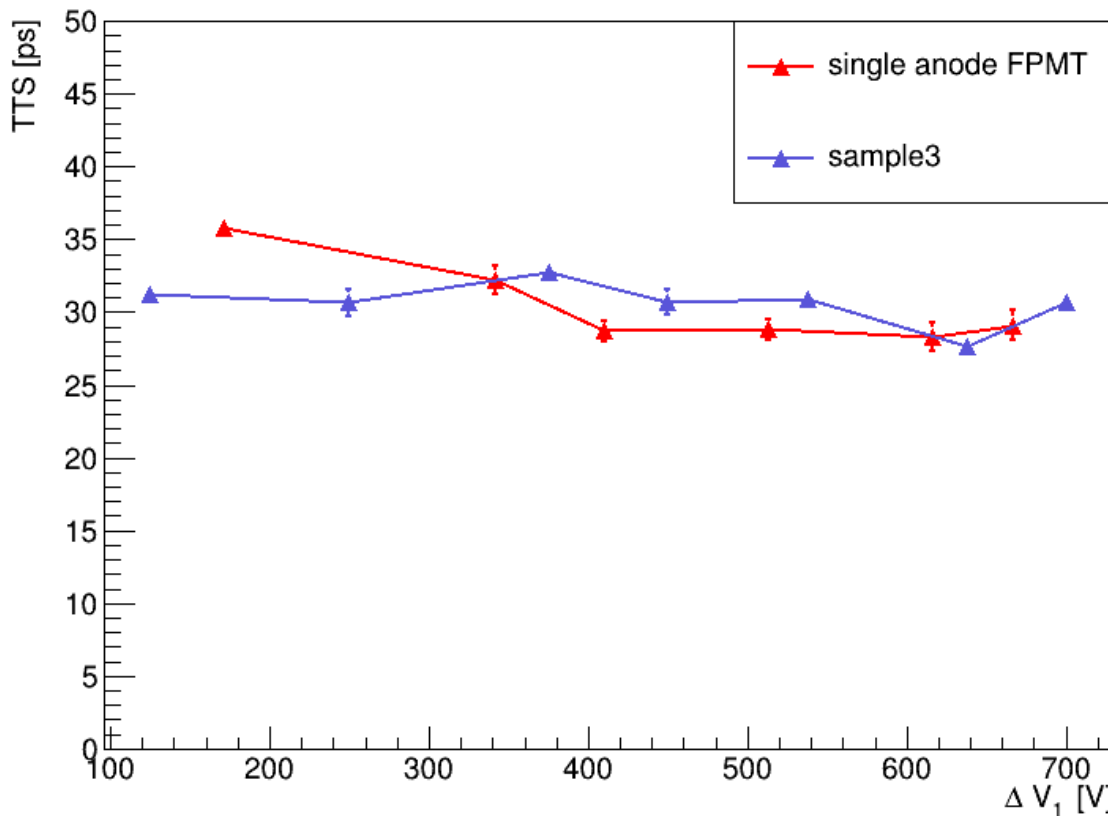


Figure 6: The TTS of sample3 changed with ΔV_1 compared to the previously reported single anode FPMT.

4. Conclusion

The variation in the time performance of three FPMTs with the voltage division was tested. Each of the FPMTs shows a ultra-fast time performance with a time resolution of less than , and the best one can reach the TTS of 30.7 ± 0.7 ps. The FPMTs show an insensitivity to the change of voltage division, which is because the space of cathode-MCP-anodes is small enough. Therefore, the voltage division of the FPMT can be adjusted to achieve a lower operating voltage while maintaining a gain of 10^6 , which can result in a lower dark rate and a high security.

Acknowledgements

Sincere gratitude goes to Shuyue Zhang from Choate Rosemary Hall. The tests and analysis she conducted during her summer internship were of great importance for this article.

References

- [1] K. Gofron and N. Duke, *Using x-ray excited uv fluorescence for biological crystal location*, *Nuclear Instruments and Methods in Physics Research Section A: Accelerators, Spectrometers, Detectors and Associated Equipment* **649** (2011) 216.

- [2] R. Ota, K. Nakajima, I. Ogawa, Y. Tamagawa, H. Shimoi, M. Suyama et al., *Coincidence time resolution of 30ps fwhm using a pair of cherenkov-radiator-integrated mcp-pmts*, *Physics in Medicine Biology* **64** (2019) 07LT01.
- [3] H. Wang, W. Su and M. Tan, *Endogenous fluorescence carbon dots derived from food items*, *The Innovation* **1** (2020) 100009.
- [4] J. Wu, C.S. Tan, H. Yu, Y. Wang, Y. Tian, W. Shao et al., *Recovery of four covid-19 patients via ozonated autohemotherapy*, *The Innovation* **1** (2020) 100060.
- [5] S. Qian, W. Qi, C. Yiqi, C. Pengyu, H. Guorui, J. Muchun et al., *The mass production and batch test result of the 15K 20-inch MCP-PMT in NNVT for JUNO*, in *Proceedings of 40th International Conference on High Energy physics — PoS(ICHEP2020)*, vol. 390, p. 771, 2021, DOI.
- [6] on behalf of the MCP-PMT workgroup, Q. Wu, Y. Cao, G. Huang, Z. Hua, M. Jin et al., *Ramp;d of ultra-fast 8 × 8 anodes mcp-pmt*, *Journal of Instrumentation* **17** (2022) T04002.
- [7] J.S. Milnes and J. Howorth, *Picosecond time response characteristics of microchannel plate PMT detectors*, in *26th International Congress on High-Speed Photography and Photonics*, D.L. Paisley, S. Kleinfelder, D.R. Snyder and B.J. Thompson, eds., vol. 5580, pp. 730 – 740, International Society for Optics and Photonics, SPIE, 2005, DOI.
- [8] Y. Zhu, S. Qian, Q. Wu, G. Zhang, L. Ma and Z. Wang, *Study on fast timing mcp-pmt in magnetic fields from simulation and measurement*, *Sensors and Actuators A: Physical* **318** (2021) 112487.
- [9] L. Ma, G. Huang, Z. Hua, M. Jin, Z. Jin, S. Liu et al., *R d of a novel single anode fast timing mcp-pmt*, *Nuclear Instruments and Methods in Physics Research Section A: Accelerators, Spectrometers, Detectors and Associated Equipment* **1041** (2022) 167333.
- [10] S. Qian, L. Ma, H. Guo, G. Huang, Q. Hu, Z. Li et al., *The status of the R&D of Ultra Fast 8 times 8 Readout MCP-PMTs in IHEP*, *PoS ICHEP2020* (2021) 867.
- [11] L. Ma, S. Qian, Z. Ning, Z. Wang, Y. Zhang, Y. Zhu et al., *How to improve the performance of fast timing detector*, *IEEE Transactions on Nuclear Science* **68** (2021) 2459.
- [12] L. Ma, L. Chen, P. Chai, Z. Liang, G. Huang, J. Hu et al., *A novel multi-anode mcp-pmt with cherenkov radiator window*, *Nuclear Instruments and Methods in Physics Research Section A: Accelerators, Spectrometers, Detectors and Associated Equipment* **1049** (2023) 168089.
- [13] J. Xie, M. Demarteau, E. May, R. Wagner and L. Xia, *Fast-timing microchannel plate photodetectors: Design, fabrication, and characterization*, *Review of Scientific Instruments* **90** (2019) 043109.
- [14] Z. Li, X. Li, P. Chen, C. Li, Y. Wei, X. Sai et al., *Test of a novel 2* 2 multi-anode mcp-pmt*, *Radiation Detection Technology and Methods* **4** (2020) 472.

Full Authors List: the MCP-PMT workgroup

Lingyue Chen^{1,3}, Sen Qian¹, Shuyue Zhang⁴, Guorui Huang², Zhehao Hua¹, Muchun Jin², Zhen Jin², Lishuang Ma¹, Ling Ren², Shuguang Si², Jianning Sun², Qi Wu^{1,3}, Xingchao Wang², Yifang Wang^{1,3}, Zhi Wang², Ning Wang², Kai Wu² and Haoda Zhang²

¹Institute of High Energy Physics, Chinese Academy of Sciences,
100049 Beijing, China.

²North Night Vision Science & Technology (Nanjing) Research Institute Co. Ltd,
211100 Nanjing, China.

³School of Physical Sciences, University of Chinese Academy of Sciences,
100049 Beijing, China.

⁴Choate Rosemary Hall,
333 Christain Street, Wallingford, USA

POS (ICRC2023) 047